

Impact craters as indicators of tectonic and volcanic activity in the Beta-Atla-Themis region, Venus

Audeliz Matias
Donna M. Jurdy*

Department of Geological Sciences, Northwestern University, 1850 Campus Drive, Evanston, Illinois, 60208-2150, USA

ABSTRACT

Various features on Venus have been attributed to plumes or diapiric upwellings: the nine regiones, broad topographic rises extending thousands of km; approximately two hundred radial graben-fissure systems, extending hundreds of km; and three- to five hundred quasi-circular coronae with an average diameter of ~250 km. For each of these structures, alternative explanations have been proposed. Venus hosts nearly one thousand impact craters, which indicates that the planet was resurfaced ca 750–300 Ma; the presence of dark parabolic deposits provides age estimates for some craters. A minority of craters has been modified by tectonic and/or volcanic activity. Using the impact crater distribution and modification, we assess competing explanations for each of the suggested plume-related features in the Beta-Atla-Themis (BAT) region. The BAT region includes the planetary geoid and topographic highs, profuse volcanism, the intersection of three major rifts, and numerous coronae. Furthermore, although the BAT region covers just one-sixth of the surface, it contains 61% of the craters that are both tectonized and embayed. Using Magellan radar and altimetry data to establish uplift and deformation, detailed interpretations are given for six craters: three for Atla Regio (Uvaysi, Piscopia, Richards) and three for Beta Regio (Truth, Sanger, Nalkowska). Most impact craters dip away from Atla's geoid high, but on Beta, dip directions are more random, which may indicate that Atla is younger and more active than Beta. Within radial systems, minimal volcanic modification of craters has occurred, and crater dips do not suggest recent uplift. Modification and deficit of craters near and within coronae indicate that volcano-tectonic processes, possibly plumes, form them and may still be active.

Keywords: Venus, impact craters, plumes, coronae, radiating swarms

INTRODUCTION

Unlike Earth, Venus apparently lacks plate tectonics. Thus plumes may be an important mechanism for heat transport on our sister planet (Phillips and Malin, 1983). A variety of features

at different scales has been attributed to plume or diapiric activity on Venus. Examples of these include broad topographic swells or the regiones (Solomon et al., 1991; Smrekar et al., 1997), radiating graben-fissure systems (Grosfils and Head, 1994; Ernst et al., 2003), and coronae (Stofan et al., 1992). Stofan and

*E-mail: donna@earth.northwestern.edu.

Smrekar (this volume) examine various features on Venus as possible thermal upwellings: topographic rises, coronae, large flow fields, and also large volcanoes. They conclude that surface evidence on Venus supports the existence of about the same number of large upwellings as on Earth, but in the absence of disruptive earthlike plate tectonics, small-scale (or what they term “secondary plumes”) dominate. In an alternative interpretation of coronae origin, Hamilton (this volume) argues that very early impacts caused these structures rather than recent diapiric upwellings, and that the planetary surface is correspondingly ancient.

Field study of Venus’ surface is not possible. Thus we make use of impact craters to study proposed plume or diapiric-related features there. In this paper, we consider structures at three different scales that have been attributed to plumes on Venus: large topographic rises, or regiones, extending thousands of km; fissure or dike systems, radiating hundreds of km; and the three- to five hundred circular constructs termed *coronae*, with diameters generally of 100–300 km. The processes forming these diverse structures on Venus remain unclear; however, the formation of impact craters is well understood (Melosh, 1989). The number of craters on Venus’ surface approaches one thousand, and they are nearly randomly distributed. The modification of a crater or its ejecta by disruption or embayment by lava from outside documents local tectonic and/or volcanic activity, and the parabolic deposits associated with some craters give their approximate age, thus dating activity. Also, dip of the crater floor, which initially forms flat, indicates later reorientation (Connors, 1992). Thus we argue that the analysis of impact craters has the potential to provide clues about the timing, extent, and nature of tectonic and volcanic processes. This analysis, then, will give further insights into the existence of diapirs or plumes on Venus.

Venus’ surface seems to have undergone a resurfacing event 750–300 Ma, based on impact crater density (Phillips et al., 1992; Schaber et al., 1992; Namiki and Solomon, 1994; Mc-

Kinnon et al., 1997). Of the 940 impact craters cataloged by Phillips et al. (1992) on Venus, 158 have been tectonized only (17.6%), 55 embayed only (6.1%), and 19 have been unambiguously both tectonized and embayed (2.1%). However, the majority of craters (74.2%) remains in pristine condition. In general, Venusian craters exhibit central peak(s), wall terracing, and flat floors, characteristic of complex craters (Phillips et al., 1991). To a first approximation, craters show a random distribution over the planetary surface (Phillips et al., 1992; Schaber et al., 1992), but statistical analysis reveals a deficit of approximately fifteen or twenty craters near the rift zones (Stefanick and Jurdy, 1996). Moreover, the plains and shield fields contain a high crater density with a lower proportion of altered craters (Price and Suppe, 1995).

A distinctive occurrence on Venus is the presence of approximately sixty parabola-shaped deposits first identified in Pioneer images by Pettengill et al. (1980). These parabolas enclose a crater at the focus, and all open toward the west. Campbell et al. (1992) explained the parabolas as the result of the interaction of fine ejecta material with the zonal east-to-west winds, and they classified the parabolic types into five groups: dark, adivar, open, bright, and emissivity. Dark and bright parabolas refer to dark and bright parabolic deposits, respectively, as seen in the radar images. The adivar type, characterized by the crater Adivar, is defined as a “parabolic radar-dark deposit surrounded by a larger parabolic radar-dark deposit” (Campbell et al. 1992, p. 16,253). If the parabolic dark deposit contains an internal parabolic region with no apparent deposit, it is classified as “open.” However, a parabolic deposit more visible as an area of low emissivity is classified as “emissivity.” Atla Regio contains six paraboloidal craters (Fig. 1): four dark, one open, and one adivar. Unfortunately, none of these types of craters occurs on Beta Regio. Based on stratigraphy, Basilevsky (1993) and Basilevsky and Head (1998) concluded that the parabola-associated craters are contemporaneous with the latest stages of

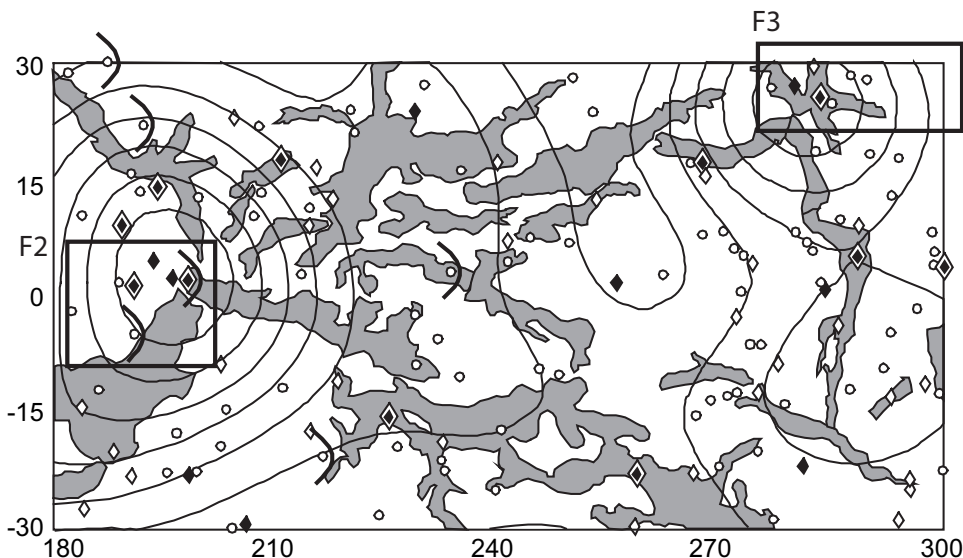


Figure 1. The Beta-Atla-Themis region, showing geoid and craters. Location of pristine craters (open circles) and modified craters (open diamond—tectonized; solid diamond—embayed; double diamond—both tectonized and embayed). Parabola-associated craters indicated with a dark parabolic symbol. Rift zones as defined by Price and Suppe (1995) shown in gray; contours for 10 m of geoid, degree 10. F2 and F3 correspond to the areas shown in Figures 2 and 3, respectively.

rifting at ca. 50 Ma, the most recent activity on Venus. Hence these parabolic craters are thought to be among the youngest 10% of craters on the planet (Campbell et al., 1992; Basilevsky, 1993; Schaller and Melosh, 1998). Consequently the presence and degree of modification of craters with these deposits can serve as markers for dating tectonic and/or volcanic activity.

We used radar images of craters to interpret their morphology, evolution, and features (e.g., ejecta, faults, volcanic episodes) in the Beta-Atla-Themis (BAT) equatorial region. In addition, we best-fit planes to the altimetry data to establish the dips of craters ≥ 15 km to compare to the regional dips. The direction of crater outflow, if present, provides an independent record of local dip at the time of impact. We assume that this outflow direction also represents regional dip. Any discordance in dips between crater interior and surroundings or outflow direction indicates local deformation. Under special conditions of multiple radar coverage, some features can be resolved with very-high-resolution topography, providing detailed mappings of the crater interiors and ejecta. Using this approach, we consider proposed plume-related features using crater densities, modification, and orientation to establish the location and timing of tectonic and volcanic activity. First, we examine impact craters on Beta and Atla to compare the level and timing of activity on these regions. Second, using some of the craters in these areas, we compare two possible models—the plume uplift and the alternative dike swarm hypotheses—for the numerous radiating graben-fissure systems on Beta. Last, we consider crater density and examine dip and modification of craters in areas of coronae to discriminate between models for their origin and evolution.

BAT Region

In our study we focus on the BAT region ($\pm 30^\circ$ N, 180° – 300° E), the intersection of three rift zones defined in the global map of Venus (Price and Suppe, 1995) (Fig. 1). These three rift arcs extend through: (1) Aphrodite-Beta zone from 25° S, 150° E to 25° N, 280° E; (2) Themis-Atla from 25° N, 180° E to 40° S, 320° E; and (3) Beta-Phoebe from 40° N, 285° E to 20° S, 285° E. The BAT region most probably has been active recently and may still be active, with planetary geoid highs, profuse volcanism, and numerous coronae. Because of the high level of volcanic and tectonic activity there, it is the most likely location on Venus for plume activity. Both Beta and Atla Regions are dominated by rifts and large volcanic edifices, with Atla (Fig. 2) containing some of the largest volcanoes in the planet (e.g., Maat Mons) and Dali, Paga, Hecate, and Ganis Chasmata (Crumpler et al., 1997). On Beta Regio (Fig. 3A), Theia and Rhea Montes overlie the Devana Chasma. Coronae, abundant circular features on Venus, were first identified in radar images well before the Magellan mapping (Barsukov et al., 1986) and were later mapped and cataloged from Magellan images (Stofan et al., 1992). For mapping purposes, coronae have been defined as circular to irregular volcano-tectonic features

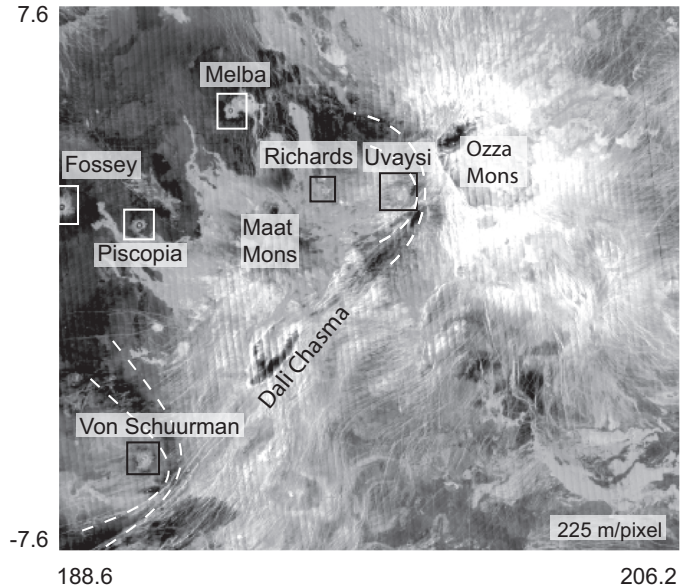


Figure 2. Central Atla Regio. Compressed mosaic image data record (C1-MIDR) radar image for the $\sim 1580 \times 1580$ km area, showing the location of craters visible in this image, volcanic edifices (Ozza and Maat Mons), and part of Dali Chasma. Latitude and longitude are shown for the region. Bright areas in radar images are relatively rough or are surfaces facing the antenna, whereas dark areas are smooth. Note the presence of dark-parabolic deposits (white dashed lines) associated with craters Von Schuurman and Uvaysi.

(Price and Suppe, 1995), interpreted to result from rising diapirs (Stofan et al., 1992). Themis Regio is dominated by coronae ranging in diameter from 200 to 500 km (Stofan et al., 1992; Smrekar et al., 1997). These three regions are part of the nine broad topographic rises interpreted as surface manifestations of mantle upwelling (Smrekar et al., 1997). The BAT region as defined contains 153 impact craters: 102 pristine, thirty tectonized-only, ten embayed-only, and eleven both tectonized and embayed. Although the BAT region covers just one-sixth of the planetary surface, fully 23% of Venus' modified craters and most of its craters that have been both tectonized and embayed (61%) occur in this region (Matias and Jurdy, 2002).

ANALYSIS

For this study, we looked at Magellan's full-resolution and compressed mosaic image data records (F-MIDRs and C1-MIDRs, with resolutions of 75 and 225 m/pixel, respectively). The Magellan mission to Venus from 1990 to 1994 proved to be a great success. The Magellan radar system operated in three different modes: Synthetic-Aperture-Radar (SAR) imaging, nadir-directed altimetry, and thermal emission radiometry (Pettengill et al., 1991; Saunders et al., 1992). Pettengill et al. (1991), Saunders and Pettengill (1991), Saunders et al. (1992), Ford (1993), and Ford and Plaut (1993) discussed in great detail the mission radar system and data products. During the first three cycles,

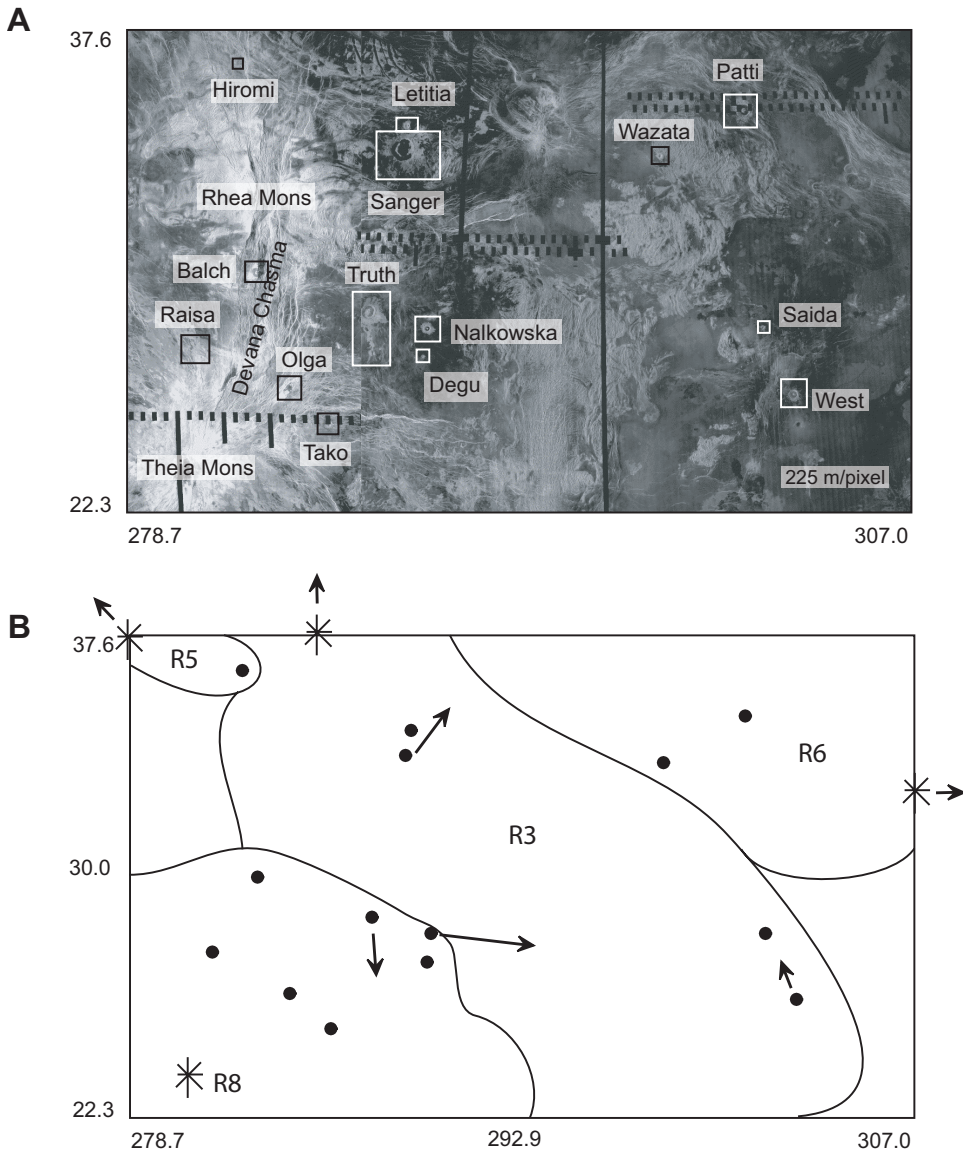


Figure 3. Eastern Beta Regio. (A) Compressed mosaic image data record (C1-MIDR) radar mosaic of the region ($\sim 3160 \times 3160$ km), with fourteen visible craters. Devana Chasma, a major rift, extends north-south with a volcanic edifice (Theia Mons) superimposed. Black vertical lines are data gaps, each ~ 20 km wide. (B) Craters shown as filled circles, corresponding to identification in (A). Dip directions for selected craters shown with arrows approximately scaled by length. Fields are shown for numbered radiating systems, centers given with asterisks (Ernst et al., 2003).

98% of the planetary surface was mapped using radar. This mapping provided the first global, high-resolution (~ 100 m/pixel) map of Venus (Saunders et al., 1991; Ford and Plaut, 1993). Many areas were mapped more than once with different illumination angles and/or directions. For more detail about incidence angles and spatial resolution see Plaut (Table 4.1 in 1993), and Ford and Plaut (Table 2-1 in 1993), respectively.

We have derived generalized surficial geology maps from the high-resolution radar images. The maps represent the interpreted morphological units as resolved from the reflectivity and topographic changes on the images. The main components identified include crater cavity, ejecta blanket, central peak(s), wall terracing, and, occasionally, outflow. Also, using Magellan altimetry, we best-fit topography with dipping planes to assess the local tilt; the altimetry has 10–20 km horizontal resolution (Ford and Pettengill, 1992).

Magellan radar-mapped Venus with three cycles at different incidence angles, with multiple cycle coverage over the surface, so that stereo imaging can be undertaken to obtain high-resolution topography (Plaut, 1993). Using the incidence angles for both images, elevation can be obtained by the parallax:height ratio on opposite-side or same-side stereo images. Stereo imaging exceeds altimetry resolution by a factor of ~ 100 (Plaut, 1993). To obtain high-resolution topography from possible stereo-radar pairs, we used the software package Magellan Stereo Toolkit (MST) version 2.0 (Vexcel Corporation, Boulder, CO) that we have implemented in batch mode. Herrick and Sharpton (2000, p. 20,247) created stereo-imaged topography for Venus' impact craters and estimated the vertical resolution as "potentially a few tens of meters, but realistically is ~ 100 m." Unfortunately, the entire planet was not imaged by all three cycles. Indeed, of the 153 craters in the BAT region, only thirteen craters have two-

TABLE 1. SUMMARY OF CRATERS DISCUSSED

Crater name	Latitude (° N)	Longitude (° E)	Diameter (km)	Regio	Modification	Description
Uvaysi	2.3	198.2	38.0	Atla	TE, Pa	Young, with severe modification
Von Schuurman	-5.0	191.0	28.9	Atla	Pr, Pa	Young, without modification
Piscopia	1.5	190.9	24.8	Atla	TE	Cavity details stereo-imaged; region dips 0.24° W; interior dips 0.17° WSW
Richards	2.5	196.1	22.2	Atla	E	Multiple episodes of embayment; region dips 0.57° N; interior dips 0.30° SW
Truth	28.7	287.8	46.1	Beta	Pr	On R8* lineament; both region and interior dip ~0.19° S; outflow also dips to the S
Sanger	33.8	288.6	83.8	Beta	Pr	On R3 lineament, both region and interior dip ~0.18° NE
Nalkowska	28.1	290.0	21.1	Beta	Pr, Fh	On R8 lineament; region dips 0.35° E, but crater interior is flat
Bashkirtseff	14.7	194.1	36.7	Atla	TE	Multiple episodes of embayment; region dips 0.21° SW
Raisa	27.5	280.3	13.0	Beta	TE	On R8; only embayed crater on the radiating systems
Balch	29.9	282.9	39.4	Beta	T	On R8; offset by Devana Chasma
West	26.1	303.0	28.0	Beta	Pr	On R3 lineament; region dips 0.06° NW
Cholpon	40.0	290.0	5.6	Beta	T	On R3 lineament
Martinez	-11.7	174.7	23.1	Atla	T	On a middle-stage corona; dips 0.39° WSW
Warren	-11.7	176.5	49.4	Atla	TE	On a middle-stage corona
Aethelflaed	-18.2	196.6	18.4	Atla	Pr	On the rim of an old-stage corona dipping to the E;† region dips 0.27° SSW; interior nearly flat
Ketzia	4.0	300.5	14.5	Beta	TE	On a middle-stage corona; both region and interior dip ~0.20° SW

Note: Craters are listed in the order they are mentioned in the text. The coordinates and diameters correspond to Herrick et al. (1997); modification according to our interpretation. Abbreviations: E—embayed only; Fh—faint remnants of a dark halo deposit; Pa—parabola associated deposit; Pr—pristine; T—tectonized only; TE—both tectonized and embayed.

*Radial graben-fissure system, Ernst et al. (2003) classification.

†From Stoddard and Jurdy (2003).

cycle coverage and just one crater (Warren; diameter, 49.4 km) has three-cycle coverage.

Venus' craters have been characterized by several catalogs. As noted, Campbell et al. (1992) divided fifty-seven paraboloidal craters into five types, according to their radar and emissivity characteristics. Schaller and Melosh (1998) developed a model for parabola formation confirming the Campbell et al. (1992) classification, adding one more crater to the list. General databases presenting crater name, coordinates, diameter, type, and modification stage are given independently by Phillips et al. (1992) and Schaber et al. (1998). Independently, Herrick et al. (1997) compiled a more detailed listing of all craters, including such characteristics as continuous ejecta radius and rim completeness. In addition, Collins et al. (1999) reevaluated the crater population believed to be embayed, finding that it comprises ~3–6% of the total, and that most are embayed by the youngest phase of volcanism. Finally, large impact craters (diameter \geq 30 km) and basins were discussed by Alexopoulos and McKinnon (1994); they measured ring spacing and grouped craters by peak-ring types. For our study, although we have independently evaluated the degree and type of modification of each crater, we adapt the crater catalog by Herrick et al. (1997) for locations, sizes, and modification.

The following six examples of the 153 craters located in the BAT region were selected for detailed analysis because of their proximity to the geoid peak, within 30 m (3 contours). Figures 2 and 3A show C-MDIR images for Atla and Beta, respectively,

with crater locations. Note the presence on Atla (Fig. 2) of two craters, Uvaysi and Von Schuurman, with associated parabolic deposits. In Figure 3B, we show the dips of selected craters. Craters discussed in this paper are summarized in Table 1.

Atla Regio Crater Examples

Uvaysi. Previously known as Luxemburg, this crater lies at the intersection of Dali, Ganis, and Parga Chasmata (2.3° N, 198.2° E) on Atla Regio (Fig. 2). Phillips et al. (1992) and Herrick et al. (1997) are in agreement that this crater has been modified strongly by lavas and is thus considered embayed; additionally, Phillips et al. (1992) also classified Uvaysi as tectonized. However, a later reexamination by Collins et al. (1999) showed that this 38.0-km crater (Fig. 4A) has not been embayed by lava flows from the exterior, a requirement, they argue, for classification as embayed. Importantly, Uvaysi shows a radar-dark parabola-associated deposit extending ~700 km in length and 760 km in width (Campbell et al., 1992). As noted, this association ranks the crater as among the youngest on the planet, serving to establish the timing of tectonic and volcanic modification as recent.

Magellan radar images reveal a crater with a central peak, wall terraces, and flat floor with some knobby hills (Fig. 4B). Located on the pl unit, defined as “plains with distinct flow morphology preserved” (Price, 1995), Uvaysi has a degraded central peak, as well as diffuse crater rim crest and ejecta deposits

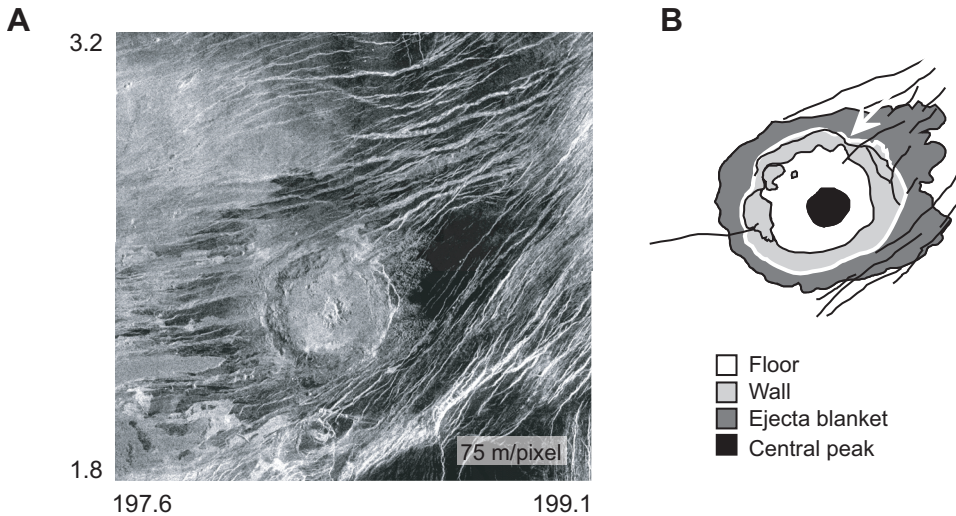


Figure 4. Crater Uvaysi (2.3° N, 198.2° E; diameter, 38.0 km). (A) East-looking Magellan radar mosaic. (B) Surficial geology map interpreted from the radar mosaic. Tectonic disruption of the crater is marked by solid black lines, and the white circle outlines the crater rim. Crater ejecta is strongly embayed on the west-southwest side, but it is not possible to identify episodes of individual flows. The rupture on the northeast rim (white arrow) perhaps provided a breach for lava flows.

(Fig. 4). A break in the rim crest, the blocky nature of the crater floor and rim, the nearly indiscernible ejecta blanket, and the presence of nearby Ozza Mons and Maat Mons (Fig. 2) all suggest embayment by lava. The rupture of the northeastern side of the rim crest, marked with a white arrow in Figure 4B, may have provided the breach where the lava flows could flood the crater's floor (Matias and Jurdy, 2002). Disruption of the crater ejecta and wall are apparent on the west side of the crater. The clear evidence of modification and the presence of an associated parabola with Uvaysi constrain the volcanism and tectonism in this area to within the last 10% of the surface history. Because of the disruption of the crater ejecta, we were unable to distinguish the crater from its surroundings with the altimetry data. Similarly, stereo imaging analysis using Cycles 1 and 2 radar images was unsuccessful due to low backscattered differences

between areas in the image. Thus we were not able to estimate the dip of the crater and its immediate surroundings or to undertake further high-resolution analysis of deformation.

Richards. Located at the peak of Atla's geoid high (2.5° N, 196.1° E; diameter, 22.2 km), Richards has been cataloged as heavily embayed by Phillips et al. (1992), Herrick et al. (1997), and Collins et al. (1999). In our interpretation, the difference in backscattered illumination in the radar image documents two major episodes of embayment: the northeastern and southwestern portions of the crater have suffered encroachment of lava (Fig. 5). Presumably, the interior of Richards was flat at the time of impact, but currently dips 0.30° to the southwest. However, the region around the crater dips strongly to the north at an angle of 0.57° . This discordant dip implies at least two episodes of regional tilting, which may correlate with the inferred stages

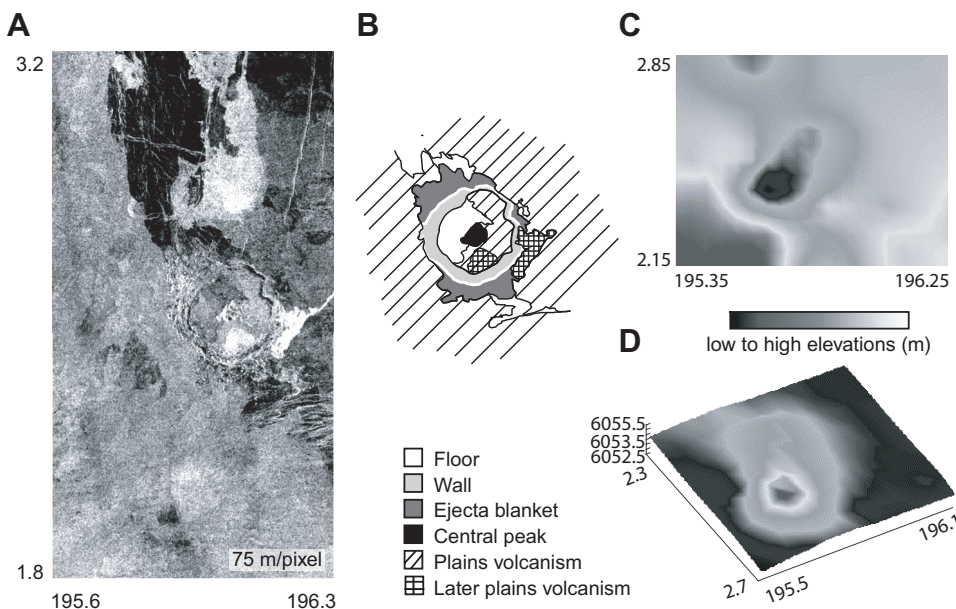


Figure 5. Crater Richards (2.5° N, 196.1° E; diameter, 22.2 km). (A) East-looking Magellan radar mosaic. (B) Surficial geology map interpreted from the radar mosaic. Difference in backscattered illumination inside and outside the crater may reflect different episodes of embayment; we established at least two. White circle outlines the crater rim. (C) Magellan altimetry data. (D) Inverted plot of altimetry data. Numbers to the left are elevations in meters. We invert to better examine the crater floor.

of embayment. The northeastern crater wall shows deformation (Fig. 5) and so may also be tectonized. Better topographic resolution is not possible. Single radar coverage of the crater prohibits stereo imaging and limits analysis to the altimetry resolution (~ 10 km). Thus we cannot unambiguously classify Richards as tectonized in addition to its obvious embayment, but its discordant tilt relative to its surroundings suggests local tectonic activity in addition to the obvious embayment, which may have occurred in several episodes.

Piscopia. This ~ 25 -km diameter crater on Atla (1.5° N, 190.9° E) has been diversely classified as both tectonized and embayed (Phillips et al., 1992), slightly embayed (Schaber et al., 1992), and even pristine (Herrick et al., 1997) (Fig. 6A). Located on the pwr unit, defined as “plains with wrinkle ridges” (Price, 1995), this well-defined crater displays a prominent central peak, continuous ejecta blanket, and flat cavity floor. Figure 6C and D show topography for Piscopia as obtained from the Magellan altimetry data. In addition, because of coverage by two radar cycles, we were able to produce high-resolution inverted topography by stereo imaging (Matias et al., 2004). We inverted

the crater as a means to reveal detailed structure of the floor, thus creating a cast or mold of the interior shape. Note the detail in the crater cavity, showing disruption in the northern and western crater wall (Fig. 6E) not apparent in Figure 6C and D, showing the Magellan altimetry. There appears to be evidence both in the radar and the altimetry that the crater suffered deformation, thus we classified it as tectonized in addition to embayed. The surrounding region dips 0.24° to the west, but the crater itself is flatter (0.17°) and dips westsouthwest. This observation suggests that, although the area had been tilted before the formation of Piscopia, the uplift has not continued after the time of impact.

Beta Regio Crater Examples

Truth. This 46.1-km diameter crater at 28.7° N, 287.8° E on Beta Regio, east of Devana Chasma (Fig. 3A), has been listed in all classifications as pristine and is notable for having a prominent radar-bright flow feature to the south (Fig. 7A). The slightly high backscattered material, called *outflow*, has been found in at least one hundred craters on Venus; these outflows are thought

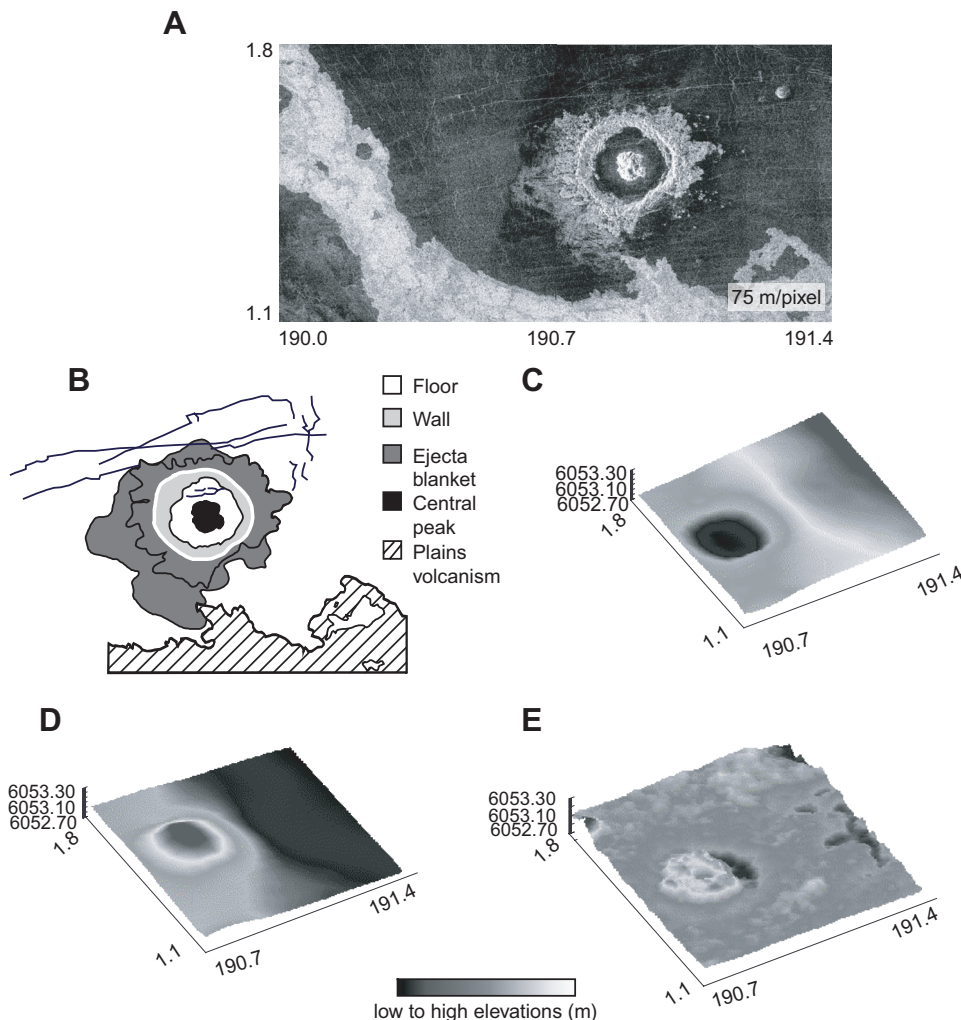


Figure 6. Crater Piscopia (1.5° N, 190.9° E; diameter, 24.8 km). (A) East-looking Magellan radar mosaic. (B) Surficial geology map interpreted from the radar mosaic. White circle outlines the crater rim. (C) Magellan altimetry data. (D) Inverted Magellan altimetry data. (E) Inverted topography derived from stereo imaging using the Magellan Stereo Toolkit (automatching mode, level 4).

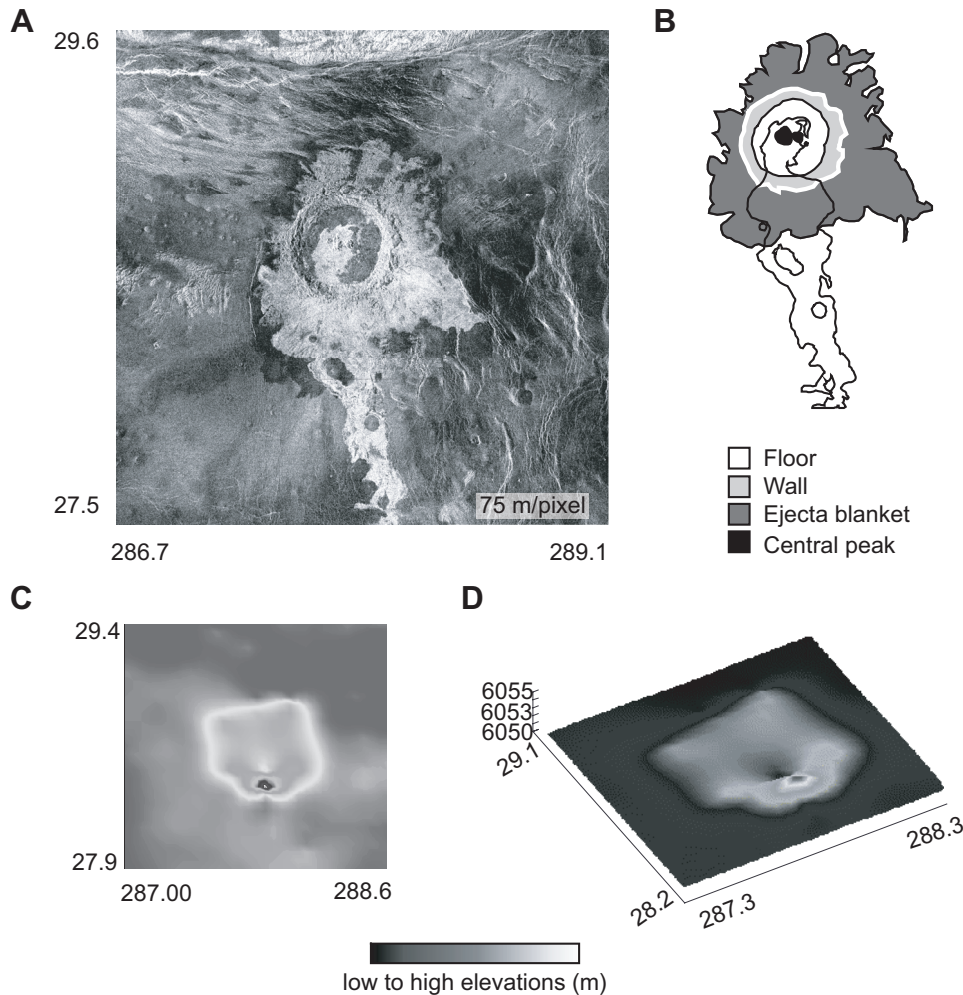


Figure 7. Crater Truth (28.7° N, 287.8° E; diameter, 46.1 km). (A) East-looking Magellan radar mosaic of nine full-resolution mosaic image data records (F-MIDRs). (B) Surficial geology map interpreted from the radar mosaic. Black line on the south encompasses the out-flow. White circle outlines the crater rim. (C) Magellan altimetry data. (D) Inverted Magellan altimetry shown as in Figure 5.

to be contemporaneous with cratering (Asimow and Wood, 1992; Chadwick and Schaber, 1993; Weitz, 1993). Schultz (1992) notes the importance of impactor direction on the initial flow, but confirms from laboratory experiments that local slope ultimately controls the flow path. In the case of Truth, the outflow extends ~ 3.5 times the crater diameter (~ 160 km) from the crater rim, as estimated using Magellan radar images. It seems to emanate from within the central peak area of Truth, although many other outflows of Venusian craters have been identified as originating from the crater rim (Asimow and Wood, 1992). The flow direction resembles the current dip direction, 0.19° to the south. Because outflows extend away from their sources and down topographic gradients (Asimow and Wood, 1992), they independently record the prevailing regional dip direction at the time of crater formation. Thus the agreement of Truth's outflow direction with the current dip of the region, in addition to the crater interior's dip (all away from Atla's center), suggests that uplift in the area has continued subsequent to the crater formation.

Sanger. Located east of Devana Chasma (33.8° N, 288.6° E), Sanger ranks as the largest crater on Beta Regio, 83.8 km in diameter. It has been classified as a double-ring basin by Schaber

et al. (1998), a peak-ring crater by Alexopoulos and McKinnon (1994), a pristine crater by Herrick et al. (1997), but as possibly embayed by Phillips et al. (1992). Figure 8 shows a crater with a circular rim and cavity and a nonuniform ejecta blanket. Oblique impact is an unlikely cause of Sanger's nonuniform ejecta blanket, because we do not see the characteristic preferential concentration of material or a wedge-shaped "forbidden zone" in the ejecta morphology. Thus we conclude that the irregular ejecta pattern of Sanger argues for embayment from the southwest, the direction of the rift.

Crater Sanger dips 0.18° to the northeast, about the same amount and direction as the immediate surroundings dip. Sanger's floor shows faint parallel lineations (Fig. 8A), suggesting possible tectonization, but confirmation with detailed resolution was not possible because of single-radar coverage. Furthermore, Basilevsky and Head (2002) classified Sanger as a clear halo crater with outflows to the northwest. Accordingly, Sanger's age is less than $0.5 \cdot T$, where T is the mean global age of Venus' surface; thus, younger than ca. 250 Ma. Lineaments from Devana Chasma cross the outflows from this crater, suggesting that rifting in the area was active more recently than 250 Ma.

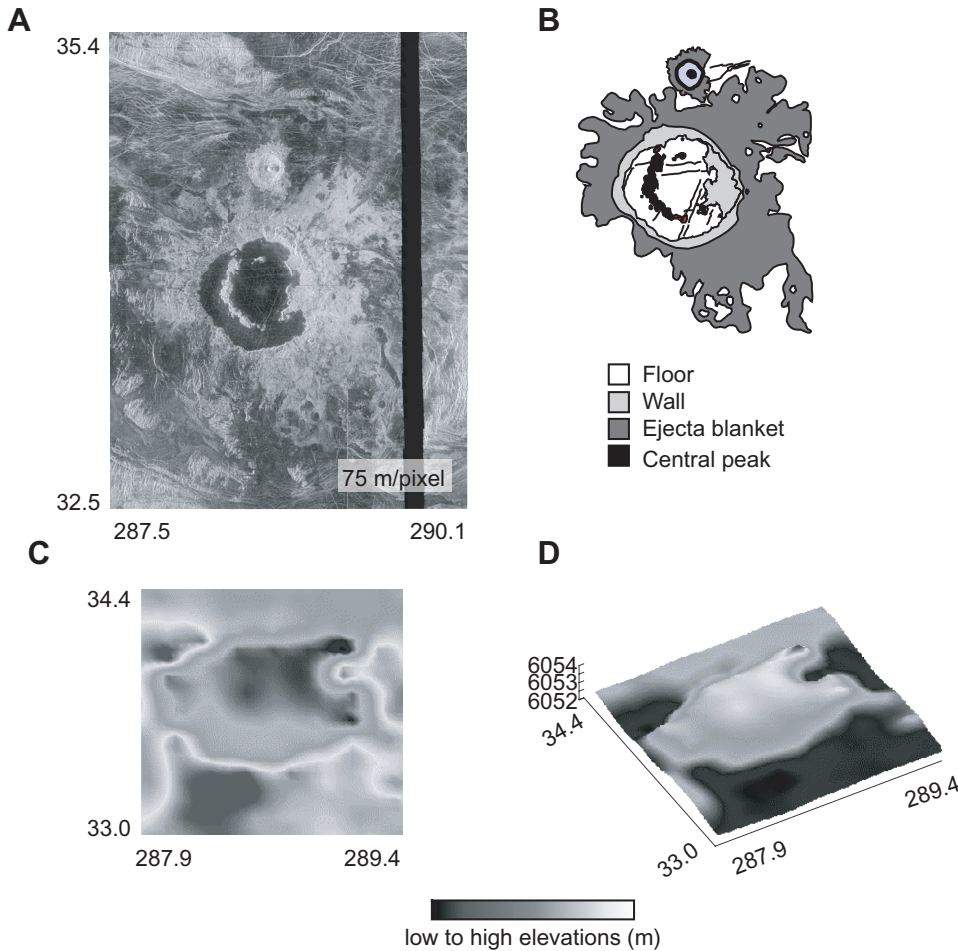


Figure 8. Crater Sanger (33.8° N, 288.6° E; diameter, 83.8 km). (A) East-looking Magellan radar mosaic of twelve full-resolution mosaic image data records (F-MIDRs). The ~ 17 -km Crater Letitia can be seen north of Sanger. (B) Surficial geology map interpreted from the radar mosaic. (C) Magellan altimetry data. (D) Inverted Magellan altimetry shown as in Figure 5.

Nalkowska. The final crater discussed on Beta Regio is Nalkowska, located at 28.1° N, 290.0° E. With no indication of tectonic or volcanic modification, this ~ 21 -km diameter crater, unanimously classified as pristine (Phillips et al., 1992; Herrick et al., 1997), has a bright-radar central peak and a dark-radar flat floor (Fig. 9). The flatness of the floor is distinctly evident in the Magellan altimetry data (Fig. 9C), with no further detail revealed in the inverted plot (Fig. 9D). However, the region exterior to the crater dips significantly (0.35°) to the east. Several radar-dark patches around the crater may be faint remnants of a dark halo. Basilevsky et al. (2003) estimated the age of 188 craters according to the degree of preservation of associated radar-dark deposits. Based on their work, craters with a faint halo of dark deposits are older than $0.5T$. Thus this undisturbed crater is not young (~ 250 Ma). Although the region around Nalkowska dips, the crater itself does not. This set of observations suggests that the regional tilting must have occurred even earlier than the impact, and this impact occurred in the first half of the surface's history. Thus uplift on Beta may be quite old. In the next section, we further discuss Nalkowska, in the context of local radiating dikes.

DISCUSSION

We studied a total of thirty-three out of ~ 150 impact structures (including the six discussed in detail above) located in the BAT region. The size distribution (diameter) of the craters examined is: one crater ≤ 15 km; sixteen craters 15–30 km; eight craters 30–45 km; and eight craters ≥ 45 km. Impact craters smaller than ~ 15 km in diameter cannot be resolved from Magellan altimetry, but very few of these exist, due to Venus' thick atmosphere, which blocks them. Location limits the identification of craters in the altimetry data, with those craters in the rift zones generally indistinguishable from their surroundings. Some patterns emerge from the analysis of these craters in the BAT region. For instance, among the nine craters both tectonized and embayed, those located on Atla and Themis Regiones suffer predominantly tectonic alteration. However, craters Richards and Bashkirtseff on Atla do show evidence of multiple episodes of embayment. In contrast, on Beta, the corresponding group of craters has experienced more embayment than tectonic disruption. Craters on Atla document its activity as recent and possibly even current; in general, Atla's craters dip away from the rift

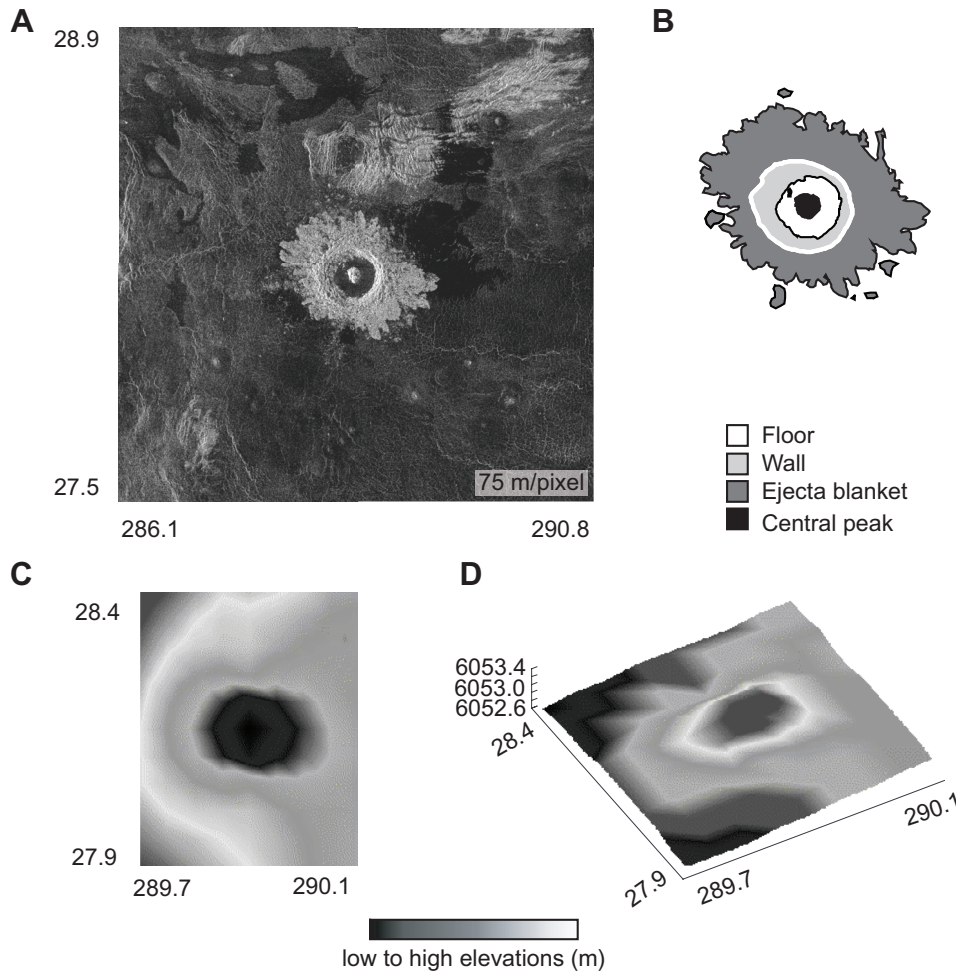


Figure 9. Crater Nalkowska (28.1° N, 290.0° E; diameter, 21.1 km). (A) East-looking Magellan radar mosaic. (B) Surficial geology map interpreted from the radar mosaic. White circle outlines the crater rim. (C) Magellan altimetry data. (D) Inverted Magellan altimetry shown as in Figure 5.

(Fig. 2). However, craters on Beta do not show the same dip pattern (Fig. 3). Beta's tilting is further discussed later in the analysis of the radiating graben systems.

Noting the nearly perfect correlation of Venus' topography with its geoid field, Sandwell et al. (1997) showed that a "swell push" body force can be calculated as the gradient of the geoid. This calculation makes specific predictions for the expected strain or deformation in the Atla and Beta Regiones, based on the values of the geoid. Both Atla and Beta show extensional strain along the rifts as the most recent tectonic deformation (Sandwell et al., 1997). Not surprisingly, the sites of the largest stress on the planet, the regiones, have many deformed craters.

Next, we consider two further tectonic applications related to the existence of smaller scale plumes or diapirs on Venus. Plumes or mantle diapirs have also been proposed to explain diverse features on Venus, including radiating dike swarms and coronae. We use the distribution, orientation, and modification of impact craters to assess plume-related models for radiating graben-fissure systems and coronae. We restrict ourselves to this tectonically active BAT region, and return to some of the same craters.

Radiating Graben-Fissure Systems

Venus' surface also hosts numerous long and narrow extensional lineaments; some are linear, some are circumferential, and others show a radiating pattern (Grosfils and Head, 1994; Ernst et al., 2003). Similar giant features have been found here on Earth. Ernst et al. (1996) and Buchan and Ernst (2004) identified 154 giant swarms, of which only ~30 (19%) are considered radiating systems (Ernst and Buchan, 2001). These giant radiating swarms have been interpreted to be dike swarms associated with the head of a mantle plume (Ernst et al., 1995), with ages from ca. 2470 to 17 Ma (Ernst and Buchan, 2001). For comparison, a classic terrestrial example of a radiating dike swarm is associated with the 1270-Ma Mackenzie plume in Canada. Here, lateral injection of magma from a central source created a fan-shaped swarm over a 100° azimuth, extending 1000 km in length.

As noted by Ernst et al. (1995), minimal weathering and erosion on Venus make it easier to study these systems than their counterparts on Earth. Grosfils and Head (1994) identified 163 large radial extensional systems over the Venus' surface and summarize the two end-member mechanisms of origin proposed

for these features. The first attributes the lineaments to a predominantly domical uplift caused by an ascending mantle diapir. They argue that this mechanism would require a central uplift and the system of lineaments limited to the extent of the uplift. A second mechanism attributes the systems to the emplacement of shallow, laterally propagating dikes out from a central magma reservoir. Unlike the mantle diapir explanation, no morphological central uplift is required by this mechanism, and the extensional features can propagate beyond the center of the system. These mechanisms represent two extremes; however, both mechanisms may have influenced some of the radial systems. Later, Ernst et al. (2003) studied in detail extensional lineaments in the northwestern Guinevere Planitia and northern Beta Regio region (24° – 60° N, 264° – 312° E). They determined the ratio of the uplift radius to the extension of the lineaments for thirty-four radiating systems, concluding that at least 32% of these radiating systems extend beyond a central uplift. Therefore they argue that dikes are a better explanation than diapirs for these radiating systems.

We consider craters to further differentiate between models for radiating graben-fissure structures. Individual craters can provide a snapshot of the nature and degree of tectonic and volcanic activity, as well as their timing at a specific location. The southern region of the Ernst et al. (2003) study area (24° – 45° N) contains five of the impact craters in our dataset (Fig. 3B). This area contains six of the giant radiating systems (R3–R8), of which five were determined by Ernst et al. (2003) to be underlain by dike swarms based on extension beyond the uplift. However, the dike swarm origin for the Theia Mons system (R8) was not advocated, because, for this system, only the topographic uplift and swarm extension radii are approximately equal. Additionally, based on overlap with other systems, they established that R8 may be the youngest in the region. Figure 3B shows approximate centers and extents for systems R3, R5, R6, and R8.

Twenty-three craters are located between 24° and 45° N, with very few showing tectonic or volcanic modification. Based on the Herrick et al. (1997) classification, this region contains two tectonized-only craters and a single crater that has been both tectonized and embayed. Using the radial system classification and mapping of lineations by Ernst et al. (2003), we defined six regions and grouped craters within each of them: five to seven in R3, two in R4, two in R5, five or six in R6, zero in R7, and seven or eight in R8. For those craters adjacent to lineaments from two systems, we assigned the crater to both. This approach differs from that of Grosfils and Head (1996), who only consider craters directly associated with lineaments and/or flows. We found little evidence of crater modification by embayment. The single crater showing encroachment by lava, Raisa (27.5° N, 280.3° E; diameter, 13 km), has been heavily embayed and also shows some tectonic disruption of its rim and ejecta. It lies ~ 400 km from the center of the R8 radiating system near a lineament (Fig. 3B). Significantly, this system is considered the youngest of the radiating-graben systems in Beta Regio (Ernst et al., 2003).

In addition, we find substantial evidence for tectonic dis-

turbance in the northern Beta region. For example, crater Balch (29.9° N, 282.9° E), also in the R8 system, serves as an excellent and often-displayed example of Venus' tectonic activity. This crater has been offset by Devana Chasma (Fig. 3A), proving that tectonic activity in the rift followed the impact. Basilevsky and Head (2002) argued that this crater does not show even the faintest dark halo, so in their estimation, Balch was formed in the earlier half of the age of Venus' surface. If the crater age is accurate, then tectonic activity could have occurred at any time going back hundreds of m.y. in the region around R8.

Crater dip or tilt may record the local uplift or subsidence history. Our analysis of dips for five craters near the highest geoid values on Beta Regio exhibits a discordant pattern. Two craters discussed for Beta Regio (Truth and Nalkowska) are located in R8, and one (Sanger) lies along a lineament of R3. Thus we can attempt to use their tilt to distinguish between either the uplift or the dike-swarm origins for these centers. Significantly, Truth (Fig. 7) displays an outflow extending south, which constrains the local topography at the moment of impact. Additionally, the crater's interior and the surrounding region both dip about the same amount, also to the south (Fig. 3B). As has been noted, this uniformity of dip directions indicates that no tectonic reorientation has occurred in that area since crater formation. Conversely, only $\sim 2^{\circ}$ east at about the same latitude, the region around crater Nalkowska (Fig. 9) shows a considerably larger dip than Truth to the east-southeast ($\sim 0.2^{\circ}$ difference), and the crater itself is flat (Fig. 3B). For active or recent uplift triggered by an ascending diapir beneath R8, we would expect both craters to dip away from the center. However, neither crater tilts away from the center of R8's lineaments. Furthermore, near R3, both the interior and surroundings of the ~ 84 -km diameter crater Sanger dip to the northeast. To the south of the R3 center, we find that Crater West (Fig. 3A) dips slightly to the northwest (Fig. 3B). Although this evidence pertains to only two craters, their orientations do not suggest recent uplift from a central diapir for R3 either. Additionally, on R3, there is a very small crater (Cholpon; diameter, ~ 6 km) classified as tectonized, but its size prohibits further interpretation.

We found no modified craters for the remaining four radiating systems (R4–R7). The presence of ten pristine impact craters documents the relative absence of volcanic and tectonic modification for these radiating-fissure systems. This observation supports the Ernst et al. (2003) rejection of a mantle diapir associated with the radiating systems R4–R7. Furthermore, the absence of embayed craters for all of these remaining systems argues against recent profuse volcanism from shallow magma reservoirs.

What do craters reveal about the origin and evolution of radiating dikes on Venus? First, the level of magmatic disturbance of craters is unexpectedly minimal. Raisa (Fig. 3A), on a lineament of R8, is the only crater that shows evidence of embayment. In view of the lack of magmatic influence on craters, the hypothesis of a central reservoir near the surface, recently supplying numerous lateral dikes of great lengths, seems unlikely.

However, some factors may influence whether dikes reach the surface, as summarized by Ernst et al. (1995): depth, pressure, and propagating speed of the dikes. Alternatively, these dikes on Venus may be ancient, with emplacement preceding the impacts. Indeed, based on crater density and stratigraphy, Grosfils and Head (1996) previously concluded that the giant radiating systems date almost back to the resurfacing event. Evidence for tectonism of craters proves that some deformation post-dates impact, but only three out of twenty-three craters are tectonized. The alternative hypothesis of domal uplift is best considered with crater orientation. Second, the dips or tilts of the craters do not show the simple pattern expected around an active or recent uplift at R3 and R8. Although it is difficult to establish a pattern with only four craters around two centers, these data suggest collapse of these systems more than it does recent uplift. Perhaps the radiating systems formed very early in the history of Venus' surface, with impacts coming later, followed by the reorientation of the craters in response to subsequent collapse or relaxation. Outflows on the 28.0-km diameter Crater West do not agree with the current dip direction of the area to the northwest. This crater may record an ancient uplift of Beta, opposite to the current stage of topographic relaxation. The same pattern is observed for Crater Sanger (Fig. 8), where outflows also run to the northwest whereas the region currently dips to the northeast.

The craters that we have studied give some tantalizing hints about the origin of radiating dikes on Venus in a limited, but tectonically active region. However, we cannot draw firm conclusions on the basis of just a handful of craters. To fully test our observation of minimal magmatic activity and of crater orientations discordant with a simple uplift model dipping away from the center of the dike system, all craters from 24° to 60° N and 264° to 312° E must be studied in detail. We only examined the southern portion of this region. Locations of volcanic and tectonic activity could be mapped by the modification of craters. Furthermore, construction of surficial geology maps is needed for critical craters, as such maps proved useful in our study. Fitting planes to the region within the crater (if large enough), as well as the region outside, could help assess the orientations of the craters. These orientations could be compared with the prediction of uplift at the centers of radiating systems. In addition, the orientation of outflow from a crater provides the dip direction at the time of impact, giving another stage of regional orientation. The presence of dark halos or remnant dark patches provides an estimate of the age of the crater, which, in turn, can time potential activity. This expanded analysis would be informative and helpful in fully characterizing the radiating-graben fissures, but it is, however, beyond the scope of our study.

Coronae

Coronae, abundant features on Venus, vary from 60 to 2600 km, with a median diameter of 230 km (Stofan et al., 1992). Consisting of a central plateau surrounded by an annular ring of ridges and troughs, a corona typically includes extensive

exterior volcanism and tectonism (Stofan et al., 1992). In their initial analysis of global coronae, Stofan et al. (1992) identified 336 coronae and twenty-six corona-like structures. Corona evolution has been envisaged as the interaction of a rising diapir with some boundary layer. This interaction predicts a variation in corona-associated volcanism and tectonic deformation throughout the evolution of the feature. During the initial domal uplift, radial fractures are formed, with volcanism limited to the corona interior. Subsequently, a flattening of the interior and development of an annular moat occurs, with volcanism prevalent outside the corona interior. Coronae evolution terminates with the formation of a central caldera (Stofan and Head, 1990; Janes et al., 1992; Stofan et al., 1992). Koch and Manga (1996) have estimated that it would take 50 m.y. for a 100-km radius diapir to evolve from an initial uplift to a caldera. However, in this volume, Hamilton presents an alternative hypothesis: that coronae are remnants of ancient eroded impact craters and do not represent rising diapirs.

To assess these alternative models for corona origin and evolution, we first review the relationship between impact crater distribution and coronae in the BAT region. Namiki and Solomon (1994) determined that there is crater deficit in corona interiors. Following this analysis, DeLaughter and Jurdy (1997) unexpectedly found a crater deficit out to four corona radii. They then classified coronae on the basis of indicated evolutionary stage from interior topography (DeLaughter and Jurdy, 1999). Furthermore, the region of geoid highs that encompasses the chasmata intersection (Fig. 1) was shown to be the area of corona concentration and deficit of craters, as well as the location of many modified craters (Stefanick and Jurdy, 1996; Jurdy and Stefanick, 1999). Thus these researchers argue that the process that generates coronae is the same one that modifies craters and ultimately eradicates them, causing the observed deficit. If, however, coronae themselves represent the sites of ancient impact craters (Hamilton, this volume), then instead, there should be a surplus of smaller craters superposed on these old regions rather than the observed deficit.

We now examine the volcanic and tectonic activities modifying craters near coronae. We considered the state and presence of craters in coronae in the BAT region. Stoddard and Jurdy (2003) note the absence of coronae near the crest of both Atla and Beta regiones. However, two middle-stage coronae located southwest of Atla's crest (within four geoid contours, or 40 m) each contain a single tectonized crater. One of these, crater Martinez (11.7° S, 174.7° E; diameter, ~23 km), displays tectonization both inside and outside its cavity, with the surroundings dipping considerably (0.39° westsouthwest). Crater Warren (11.7° S, 176.5° E; diameter, 49.4 km), classified as tectonized, also shows evidence of embayment in its interior, with part of the central peak covered. We were unable to calculate dips for this crater, as it was unclear in the topographic data. Furthermore, only one of the old-stage coronae, located south of Atla's crest, encloses a crater. Tilting measurements for the pristine crater Aethelflaed (18.2° S, 196.6° E; diameter, 18.4 km), indi-

cate that both its interior and immediate surroundings dip in the same directions (interior southsoutheast and surroundings south-southwest), but the interior is nearly flat. However, the corona dips to the east (Stoddard and Jurdy, 2003). In addition, a possible outflow extends to the north, indicating that at the time of impact, the corona topography was more domelike. The difference in the initial and present orientations of the crater suggests an early uplift and subsequent collapse of the corona. Comparing Beta Regio, we find only one middle-stage corona that has an associated crater, Ketzia (4.0° N, 300.5° E; diameter, 14.5 km). This crater has been heavily tectonized in addition to having been embayed and dips about the same ($\sim 0.2^\circ$) as its surroundings to the southwest. No other corona in Beta has a crater in its interior or immediately adjacent.

To summarize, there are very few impact craters in or adjacent to coronae for the Atla and Beta Regiones. This paucity of craters suggests their removal by the same processes forming coronae. Two middle-stage coronae in Atla Regio and one in Beta Regio have craters. All of these craters have been tectonized, and the one in Beta has also been embayed. The single pristine crater (Aethelflaed) associated with a corona overlies the rim of an old-stage corona that has caused no tectonic disruption subsequent to impact. None of the youngest-stage coronae (those with predominately raised interiors) has an associated crater in its interior or even nearby. Thus the modification of craters associated with coronae argues for the existence of long-term tectonic and volcanic activity at coronae, unlike a single, ancient impact. If coronae were all ancient impact sites, they should preserve more recent cratering events. Furthermore, the outflow record of the initial northward dip of the pristine crater Aethelflaed, as opposed to its current southward dip, may have captured the response of Venus' lithosphere to a diapir.

CONCLUSIONS

Venus has a young surface, estimated from crater densities as being 300–750 Ma (Phillips et al., 1992; Schaber et al., 1992; McKinnon et al., 1997). Evidence for tectonic and volcanic activity abounds, particularly in the BAT region. Impact craters that have suffered from tectonism and embayment by lava are strongly concentrated in this region. This concentration of modified craters, in addition to a slight deficit of craters, documents the ongoing obliteration of impact craters in this area. Furthermore, if the parabola-associated craters were indeed formed in the past 30–75 m.y., then the unambiguous embayment and tectonization of Crater Uvayasi on Atla critically establishes the timing of activity in the region as very recent.

Atla Regio contains a significantly higher concentration of modified craters (33%) than does Beta (23%). Moreover, on Atla, embayed-only craters are negligible and tectonized-only craters occur only at lower elevations. Tilting measurements for the surroundings of thirty craters in the BAT region indicate that most of the impact craters around Atla's geoid high dip away from the rift. Beta's modified craters are randomly distributed,

unlike those on Atla, where four of the craters that are unambiguously both tectonized and embayed cluster near the geoid high. Beta's geoid peak is 20 m lower than that of Atla, and craters are sparser and dip directions discordant (Figs. 1 and 3B). Additional stereo imaging of other craters could reveal further detail about activity in the BAT region. However, the application of the stereo imaging not only requires multiple radar images and adequate crater size, but also a discernable image. For instance, stereo-derived topography for Crater Uvayasi could not be obtained because of local chaotic deformation, even with its adequate size and multiple radar coverage. In the BAT region, only $\sim 10\%$ of the craters are covered by multiple cycles. In summary, based on the higher geoid, crater dips, and modification, we conclude that Atla Regio is more active and possibly younger than Beta Regio. This observation supports the results of Basilevsky and Head (2002), based on crater density and stratigraphy, that Atla's activity is more recent than that of Beta.

Venus' radiating fissure swarms have caused surprisingly little modification of impact craters. Almost all craters near the extensional lineaments remain pristine. A single embayed crater lies in the field of the radiating system, the very system that has been identified as the youngest. If shallow and recent magma sources had generated the radiating systems, then we would expect to find many more craters embayed by lava. The other scenario for the formation of radiating swarms requires an uplift caused by an ascending diapir. However, the craters in radiating systems do not dip away from the center. Instead, they dip more randomly, often toward the center of the radiating system, suggesting that it has collapsed since the time of impact. Thus the radiating systems may have formed preceding the impacts, as was concluded by Grosfils and Head (1996).

Coronae near Atla and Beta Regiones have very few impact craters adjacent to or inside their rims. Only four coronae contain craters: one tectonized and embayed, two tectonized only, and one pristine. The single pristine crater has recorded different regional dips that may document the evolution of an old-stage corona. The crater deficit in corona interiors and the adjacent region out to several radii, along with the strong evidence for tectonic modification of associated craters, argues for a tectonic rather than an impact origin for coronae. A diapir model for coronae could account for their topographic evolution, as well as crater modification, orientation, and ultimate removal.

All of these conclusions must be tentative, as we restricted our analysis to a limited region of Venus (the BAT region; $\pm 30^\circ$ latitude, 180° – 300° longitude). Each of these hypotheses should be examined in detail, globally. Specifically, our analysis of coronae and radiating fissures focused on the BAT region, known as the most volcanically and tectonically active area of the planet and not representative of Venus. Furthermore, we do not consider the possible interaction between coronae and radiating fissure swarms. Do coronae in other regions show the same modification and elimination of craters? Isolated coronae—those not under the influence of nearby regiones, volcanoes, or radiating swarms—would provide a further test of the impact theory for

coronae (Hamilton, this volume). Are radiating fissure swarms elsewhere on Venus also nearly devoid of embayed craters, an indication of limited volcanic activity? Do craters around other radiating systems indicate current or recent uplift? Or are the dips of craters similarly chaotic or random, as we observed in the Beta area? In addition, other regiones should be considered, such as volcano-dominated Bell or Dione, or corona-dominated Eistla or Themis (as classified and discussed in this volume by Stofan and Smrekar). Optimally, the effects of regiones, coronae, and radiating swarms should be distinguished, and craters used to evaluate the existence of plumes on Venus.

ACKNOWLEDGMENTS

We thank Robert R. Herrick, Kelly Maurice, and Paul R. Stoddard for their invaluable help in installing Magellan Stereo Toolkit V. 2.0 in batch mode. DJ thanks Martin Connors; a conversation with him at the Venus II conference in 1996 on the potential utility of crater orientation led to this project. In addition, we thank Sarah Andre, John E. DeLaughter, Gillian Foulger, and Paul R. Stoddard for their comments and suggestions. We also thank Eric B. Grosfils and Warren Hamilton for their comments on the first draft of this paper.

REFERENCES CITED

- Alexopoulos, J.S., and McKinnon, W.B., 1994, Large impact craters on Venus, with implications for ring mechanics on the terrestrial planets, *in* Dressler, B.O., et al., eds., Large meteorite impacts and planetary evolution: Boulder, Colorado, Geological Society of America Special Paper 293, p. 29–50.
- Asimov, P.D., and Wood, J.A., 1992, Fluid outflows from Venus impact craters: Analysis from Magellan data: *Journal of Geophysical Research*, v. 97, no. E8, p. 13,643–13,665.
- Barsukov, V.L., Basilevsky, A.T., Burba, G.A., Bobinna, N.N., Kryuchkov, V.P., Kuzmin, R.O., Nikolaeva, O.V., Pronin, A.A., Ronca, L.B., Chernaya, I.M., Shashkina, V.P., Garanin, A.V., Kushky, E.R., Markov, M.S., Sukhanov, A.L., Kotelnikov, V.A., Rzhiga, O.N., Petrov, G.M., Alexandrov, Yu.N., Sidorenko, A.I., Bogomolov, A.F., Skrypnik, G.I., Bergman, M.Yu., Kudrin, L.V., Bokstein, I.M., Kronrod, M.A., Chochia, P.A., Tyuffin, Yu.S., Kadnichansky, S.A., and Akim, E.L., 1986, The geology and geomorphology of the Venus surface as revealed by the radar images obtained by Veneras 15 and 16: Proceedings of the Lunar and Planetary Science Conference: *Journal of Geophysical Research*, v. 91, no. 4, p. D378–D398.
- Basilevsky, A.T., 1993, Age of rifting and associated volcanism in Atla Regio, Venus: *Geophysical Research Letters*, v. 20, no. 10, p. 883–886.
- Basilevsky, A.T., and Head, J.W., 1998, The geological history of Venus: A stratigraphic view: *Journal of Geophysical Research*, v. 103, no. E4, p. 8531–8544, doi: 10.1029/98JE00487.
- Basilevsky, A.T., and Head, J.W., 2002, Venus: Analysis of the degree of impact crater deposit degradation and assessment of its use for dating geological units and features: *Journal of Geophysical Research*, v. 107, no. E8, p. 5061, doi: 10.1029/2001JE001584.
- Basilevsky, A.T., Head, J.W., and Setyaeva, I.V., 2003, Venus: Estimation of age of impact craters on the basis of degree of preservation of associated radar-dark deposits: *Geophysical Research Letters*, v. 30, no. 18, 1950, doi: 10.1029/2003GL017504.
- Buchan, K.L., and Ernst, R.E., 2004, Diabase dyke swarms and related units of Canada and adjacent regions, with accompanying catalog: Québec, Geological Survey of Canada Map 2022A, scale 1:15,000.
- Campbell, D.B., Stacy, N.J.S., Newman, W.I., Arvidson, R.E., Jones, E.M., Musser, G.S., Roper, A.Y., and Schaller, C., 1992, Magellan observations of extended impact crater-related features on the surface of Venus: *Journal of Geophysical Research*, v. 97, no. E10, p. 16,249–16,277.
- Chadwick, D.J., and Schaber, G.G., 1993, Impact crater outflows on Venus: Morphology and emplacement mechanisms: *Journal of Geophysical Research*, v. 98, no. E11, p. 20,891–20,902.
- Collins, G.C., Head, J.W., Basilevsky, A.T., and Ivanov, M.A., 1999, Evidence for rapid regional plains emplacement on Venus from the population of volcanically embayed impact craters: *Journal of Geophysical Research*, v. 104, no. E10, p. 24,121–24,139, doi: 10.1029/1999JE001041.
- Connors, M., 1992, Crater floor slope and tectonic deformation on Venus: *Eos (Transactions, American Geophysical Union)*, v. 73, no. 43, p. 331.
- Crumpler, L.S., Aubele, J.C., Senske, D.A., Keddie, S.T., Magee, K.P., and Head, J.W., 1997, Volcanoes and canyons of volcanism on Venus, *in* Bougher, S.W., et al., eds., Venus II: Geology, geophysics, atmosphere, and solar wind environment: Tucson, University of Arizona Press, p. 697–756.
- DeLaughter, J.E., and Jurdy, D.M., 1997, Venus resurfacing by coronae: Implications from impact craters: *Geophysical Research Letters*, v. 24, no. 7, p. 815–818, doi: 10.1029/97GL00687.
- DeLaughter, J.E., and Jurdy, D.M., 1999, Corona classification by evolutionary stage: *Icarus*, v. 139, p. 81–92, doi: 10.1006/icar.1999.6087.
- Ernst, R.E., and Buchan, K.L., 2001, The use of mafic dike swarms in identifying and locating mantle plumes, *in* Ernst, R.E., and Buchan, K.L., eds., Mantle plumes: Their identification through time: Boulder, Colorado, Geological Society of America Special Paper 316, p. 247–265.
- Ernst, R.E., Head, J.W., Parfitt, E., Grosfils, E., and Wilson, L., 1995, Giant radiating dyke swarms on Earth and Venus: *Earth-Science Reviews*, v. 39, p. 1–58, doi: 10.1016/0012-8252(95)00017-5.
- Ernst, R.E., Buchan, K.L., West, T.D., and Palmer, H.C., 1996, Diabase (dolerite) dyke swarms of the world: Ottawa, Ontario, Geological Survey of Canada Open File 3241.
- Ernst, R.E., Desnoyers, D.W., Head, J.W., and Grosfils, E.B., 2003, Graben-fissure systems in Guinevere Planitia and Beta Regio (264°–312° E, 24°–60° N), Venus, and implications for regional stratigraphy and mantle plumes: *Icarus*, v. 164, p. 282–316, doi: 10.1016/S0019-1035(03)00126-X.
- Ford, J.P., 1993, Magellan: The mission and the system, *in* Guide to Magellan image interpretation. JPL Publication 93-24: Pasadena, California Institute of Technology, p. 1–5.
- Ford, J.P., and Pettengill, G.H., 1992, Venus topography and kilometer-scale slopes: *Journal of Geophysical Research*, v. 97, p. 13,103–13,114.
- Ford, J.P., and Plaut, J.J., 1993, Magellan image data, *in* Guide to Magellan image interpretation. JPL Publication 93-24: Pasadena, California Institute of Technology, p. 7–18.
- Grosfils, E.B., and Head, J.W., 1994, The global distribution of giant radiating dike swarms on Venus: Implications for the global stress state: *Geophysical Research Letters*, v. 21, no. 8, p. 701–704, doi: 10.1029/94GL00592.
- Grosfils, E.B., and Head, J.W., 1996, The timing of giant radiating dike swarm emplacement on Venus: Implications for resurfacing of the planet and its subsequent evolution: *Journal of Geophysical Research*, v. 101, p. 4645–4656, doi: 10.1029/96JE00084.
- Herrick, R.R., and Sharpton, V.L., 2000, Implications from stereo-derived topography of Venusian impact craters: *Journal of Geophysical Research*, v. 105, no. E8, p. 20,245–20,262.
- Herrick, R.R., Sharpton, V.L., Malin, M.C., Lyons, S.N., and Feeley, K., 1997, Morphology and morphometry of impact craters, *in* Bougher, S.W., et al., eds., Venus II: Geology, geophysics, atmosphere, and solar wind environment: Tucson, University of Arizona Press, p.1015–1046.
- Janes, D.M., Squyres, S.W., Bindschadler, D.L., Baer, G., Schubert, G., Sharpton, V.L., and Stofan, E.R., 1992, Geophysical models for the formation and evolution of coronae on Venus: *Journal of Geophysical Research*, v. 97, no. E10, p. 16,055–16,067.
- Jurdy, D.M., and Stefanick, M., 1999, Correlation of Venus surface features, and geoid: *Icarus*, v. 139, p. 93–99, doi: 10.1006/icar.1999.6089.

- Koch, D.M., and Manga, M., 1996, Neutrally buoyant diapirs: A model for Venus coronae: *Geophysical Research Letters*, v. 23, p. 225–228, doi: 10.1029/95GL03776.
- Matias, A., and Jurdy, D.M., 2002, Tectonized and embayed impact craters in the Beta-Atla-Themis region of Venus: 33rd Lunar and Planetary Sciences Conference, Houston, Texas, Abstract 1228.
- Matias, A., Jurdy, D.M., and Stoddard, P.R., 2004, Stereo imaging of impact craters in the Beta-Atla-Themis (BAT) region, Venus: 35th Lunar and Planetary Sciences Conference, Houston, Texas, Abstract #1383.
- McKinnon, W.B., Zahle, K.J., Ivanov, B.A., and Melosh, H.J., 1997, Cratering on Venus: Models and observations, in Bougher, S.W., et al., eds., *Venus II: Geology, geophysics, atmosphere, and solar wind environment*: Tucson, University of Arizona Press, p. 969–1014.
- Melosh, H.J., 1989, *Impact Cratering: A geologic process*. Oxford Monographs on Geology and Geophysics no. 11: Oxford, Oxford University Press, 245 p.
- Namiki, N., and Solomon, S.C., 1994, Impact crater densities on volcanoes and coronae on Venus: Implication for volcanic resurfacing: *Science*, v. 265, p. 929–933.
- Pettengill, G.H., Eliason, E., Ford, P.G., Liorot, G.B., Masursky, H., and McGill, G.E., 1980, Pioneer Venus radar results: Altimetry and surface properties: *Journal of Geophysical Research*, v. 85, p. 8261–8270.
- Pettengill, G.H., Ford, P.G., Johnson, W.T.K., Raney, R.K., and Soderblom, A., 1991, Magellan: Radar performance and data products: *Science*, v. 252, p. 260–265.
- Phillips, R.J., and Malin, M.C., 1983, The interior of Venus and tectonic implications, in Hunten, D.M., et al., eds., *Venus: Tucson*, University of Arizona Press, p. 159–214.
- Phillips, R.J., Arvidson, R.E., Boyce, J.M., Campbell, D.B., Guest, J.E., Schaber, G.G., and Soderblom, L.A., 1991, Impact craters on Venus: Initial analysis from Magellan: *Science*, v. 252, p. 288–297.
- Phillips, R.J., Raubertas, R.F., Arvidson, R.E., Sarkar, I.C., Herrick, R.R., Izenberg, N., and Grimm, R.E., 1992, Impact craters and Venus resurfacing history: *Journal of Geophysical Research*, v. 97, no. E10, p. 15,923–15,948.
- Plaut, J.J., 1993, Stereo imaging, in *Guide to Magellan image interpretation*. JPL Publication 93-24: Pasadena, California Institute of Technology, p. 33–43.
- Price, M.H., 1995, Dating resurfacing on Venus using impact crater densities from GIS-based global mapping [Ph.D. thesis]: Princeton, New Jersey, Princeton University, 177 p.
- Price, M.H., and Suppe, J., 1995, Constraints on the resurfacing history of Venus from the hypsometry and distribution of volcanism, tectonism, and impact craters: *Earth, Moon, and Planets*, v. 71, p. 99–145, doi: 10.1007/BF00612873.
- Sandwell, D.T., Johnson, C.L., Bilotti, F.B., and Suppe, J., 1997, Driving forces for limited tectonics on Venus: *Icarus*, v. 129, p. 232–244, doi: 10.1006/icar.1997.5721.
- Saunders, R.S., and Pettengill, G.H., 1991, Magellan: Mission summary: *Science*, v. 252, p. 247–249.
- Saunders, R.S., Arvidson, R.E., Head, J.W., III, Schaber, G.G., Stofan, E.R., and Solomon, S.C., 1991, An overview of Venus geology: *Science*, v. 252, p. 249–252.
- Saunders, R.S., Spear, A.J., Allin, P.C., Austin, R.S., Berman, A.L., Chandler, R.C., Clark, J., deCharon, A.V., De Jong, E.M., Griffith, D.G., Gunn, J.M., Hensley, S., Johnson, W.T.K., Kirby, C.E., Leung, K.S., Lyons, D.T., Michaels, G.A., Miller, J., Morris, R.B., Morrison, A.D., Piereson, R.G., Scott, X., Shaffer, S.J., Slonski, J.P., Stofan, E.R., Thompson, T.W., and Wall, D., 1992, Magellan mission summary: *Journal of Geophysical Research*, v. 97, no. E8, p. 13,067–13,090.
- Schaber, G.G., Strom, R.G., Moore, H.J., Sonderblom, L.A., Kirk, R.L., Chadwick, D.J., Dawson, D.D., Gaddis, L.R., Boyce, J.M., and Russell, J., 1992, Geology and distribution of impact craters on Venus: What are they telling us?: *Journal of Geophysical Research*, v. 97, no. E8, p. 13,257–13,301.
- Schaber, G.G., Kirk, R.L., and Strom, R.G., 1998, Data base of impact craters on Venus based on analysis of Magellan radar images and altimetry data: Reston, Virginia, U.S. Geological Survey Open-File Report 98-104, p. 29.
- Schaller, C.J., and Melosh, H.J., 1998, Venusian ejecta parabolas: Comparing theory with observations: *Icarus*, v. 131, p. 123–137, doi: 10.1006/icar.1997.5855.
- Schultz, P.H., 1992, Atmospheric effects on ejecta emplacement and crater formation on Venus from Magellan: *Journal of Geophysical Research*, v. 97, no. E10, p. 16,183–16,248.
- Smrekar, S.E., Kiefer, W.S., and Stofan, E.R., 1997, Large volcanic rises on Venus: in Bougher, S.W., et al., eds., *Venus II: Geology, geophysics, atmosphere, and solar wind environment*: Tucson, University of Arizona Press, p. 845–878.
- Solomon, S.C., Head, J.W., Kaula, W.M., McKenzie, D., Parsons, B., Phillips, R.J., Schubert, G., and Talwani, M., 1991, Venus tectonics: Initial analysis from Magellan: *Science*, v. 252, p. 297–312.
- Stefanick, M., and Jurdy, D.M., 1996, Venus coronae, craters, and chasmata: *Journal of Geophysical Research*, v. 101, no. E2, p. 4637–4643, doi: 10.1029/95JE02709.
- Stoddard, P.R., and Jurdy, D.M., 2003, Uplift of Venus geoid highs: Timing from coronae and craters: 34th Lunar and Planetary Science Conference, Houston, Texas, Abstract 2129.
- Stofan, E.R., and Head, J.W., 1990, Coronae of Mnemosyne Regio: Morphology and origin: *Icarus*, v. 83, p. 216–243, doi: 10.1016/0019-1035(90)90016-3.
- Stofan, E.R., Sharpton, V.L., Schubert, G., Baer, G., Bindschadler, D.L., Janes, D.M., and Squyres, S.W., 1992, Global distribution and characteristics of coronae and related features on Venus: Implications for origin and relation to mantle processes: *Journal of Geophysical Research*, v. 97, no. E8, p. 13,347–13,378.
- Weitz, C.M., 1993, Impact craters, in *Guide to Magellan image interpretation*. JPL Publication 93-24: Pasadena, California Institute of Technology, p. 75–92.